sciendo

POLISH MARITIME RESEARCH 2 (122) 2024 Vol. 31; pp. 13-19
10.2478/pomr-2024-0017

An Innovative Floating System with a Savonius Rotor as a Horizontal-Axis Wind Turbine

Joanna Grzelak [1]
Lara Guijarro Carrillo [2]
Jacek Nakielski [1]
Michał Piotrowicz [3]
Krzysztof Doerffer [1]
[1] Gdansk University of Technology Poland
[2] Det Norske Veritas DNV – Maritime, Spain
[3] Institute of Fluid Flow Machinery, Poland

* Corresponding author: *joanna.grzelak@pg.edu.pl (J.Grzelak)*

ABSTRACT

In this project, an innovative wind turbine was designed for a floating plant. A large Savonius rotor was replaced with a double-rotor wind turbine implemented as a horizontal-axis turbine. This double rotor was positioned on the tip of a thrust plate and fixed to the deck of a catamaran. Simple 2D numerical simulations were performed to confirm the effectiveness of the concept. An analysis of the floating system configuration was carried out, and the loads and stresses on the system components were verified. Next, floating supports with appropriate sizes were selected to counteract the forces on the wind turbine system. Finally, an anchoring system with full rotational freedom was selected for the floating platform. The present work was conducted as part of a Master's thesis.

Keywords: wind turbine, floating platform, Savonius rotor, vertical rotor, anchoring

INTRODUCTION

In recent years, there has been growing interest in offshore wind energy. Initially, fixed structure installations were used, although today, floating offshore wind turbines (FOWTs) are more common. Depending on the supporting structures used, there are several different types of bases for wind turbines. A turbine based on a jack-up platform was presented by Dymarski [1], and a design based on a tension leg platform was described by Żywicki [2]. In deeper waters, installations based on spar-type platforms are more often used [3, 4].

Devices that convert the kinetic energy of the wind into mechanical energy through rotation are known as wind turbines, which are classified according to the type of aerodynamic force that causes rotation of the blades. Turbines may be driven by aerodynamic lift or drag. Aerodynamic lift-driven turbines are considered to be high-speed devices, and have the same operating principle as the aerodynamic surfaces of aircraft. Drag-driven turbines are characterised by high torque and low speeds of operation. Depending on the arrangement of the axis of rotation, we can classify turbines as vertical- or horizontal-axis devices. The main advantage of vertical-axis turbines is that they have the ability to start in low winds [5]. In addition, the maintenance and assembly of this type are easier, since the gearbox and generator are located at ground level. These important features have inspired a great deal of research with the aim of improving the effectiveness of these wind turbines [6-10].

The simplest type of vertical turbine is the Savonius rotor model (Fig. 1), which takes the form of a hollow cylinder split in half, where the two halves are displaced to resemble an S. The inverted parts present less resistance to the wind when turning in the opposite direction, while the concave parts of the S catch the wind. However, the overpressure in the concave

areas makes it difficult for the air to escape, which negatively affects the performance of the turbine. To improve this system, it is necessary to separate the blades, leaving a gap in which there is air flow. The use of rotor segmentation can also improve the effectiveness, and was investigated for example in [11, 12].

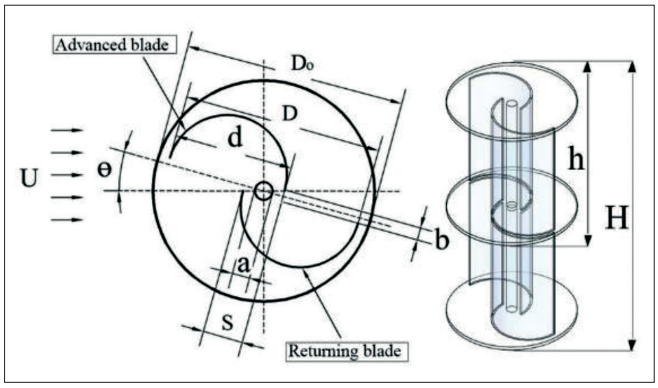

Fig. 1. Savonius rotor (from [14])

The Savonius rotor is suitable for low speeds, given the high air resistance of this type of turbine. It is therefore suitable for mechanical applications such as water pumping.

OBJECTIVE AND MOTIVATION

The importance of and growth in offshore wind energy formed the main motivation for this work. The objective of this study is to use forms of onshore wind power that have already been implemented and to put these into operation in lakes, oceans, or seas.

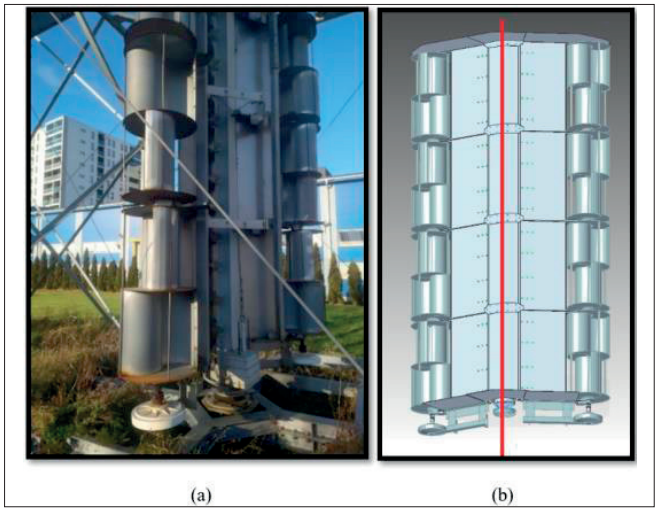

Fig. 2. (a) Example of a Savonius rotor in Centrum Techniki Okrętowej (CTO), Gdańsk; (b) the cutting process for a Savonius rotor

In this project, a large Savonius rotor is replaced with an innovative wind turbine with guide vanes and smaller rotors, as described in [13]. The system consists of a thrust plate (playing the role of a guide vane) and a rotor, and delivers as much energy as a large Savonius rotor. This new rotor design needs less material to build, meaning that it is less demanding in terms of manufacturing and costs. The system has been tested on prototypes of vertical-axis wind turbine, where both smaller rotors and guide vanes have been used. This type of wind turbine should be located in an area of water not far from the shore, with relatively shallow water, but where the wind speed is favourable for power generation.

Initially, we considered a vertical turbine consisting of guide vanes set at an angle of 60°, with eight rotors on each side (Fig. 2). However, this concept could also be implemented as a horizontal-axis wind turbine, and could work successfully either on the surface of the land or on the top of a high building, although the possibility of directing the rotors against the wind would be lost. This negative effect can be eliminated by using a floating solution, in which a floating platform is anchored to the sea bottom, allowing for 360° rotation. This innovative system adjusts itself according to the wind direction, allowing the rotors to be placed in the most efficient position to capture wind.

For the purposes of this study, we considered only half of the existing rotor (Fig. 2b). Together with the guide vane, it gave a swept area $A = H \times B = 1.25 \times 4.3\ m = 5.375\ m^2$, where B is the width and H is the height of the swept area in the new horizontal arrangement.

To achieve a platform that was highly stable and efficient, a catamaran was chosen to represent a barge platform, which was owned by Gdańsk University of Technology. The catamaran design was created in 3D using Solid Edge 2021® and its characteristics were analysed.

DESCRIPTION OF THE PROBLEM

The wind turbine considered in this project is a Savonius rotor, for which the characteristic force and power available from the wind are analysed. The characteristics are analysed for speeds ranging from zero to the winds that can be found under the action of a hurricane.

The turbine concept is implemented as a horizontal-axis wind turbine, and the possibility of directing the rotors against the wind is achieved by using a floating solution based on a catamaran composed of two pontoons, 7 m in length, made of 0.003 m 5754 H22 saltwater-resistant aluminium sheet. The diameter of each pontoon is 0.7 m, and they are divided and sealed into several modules 1.5 m long. The deck is composed of a cross-beam of type C, the main advantage being that if one module is damaged, the other modules can still be securely sealed. The total unloaded weight of the catamaran is 484 kg, and its buoyancy is 2260 N. Moulded caps are used as wall spacers to give the pontoon tubes a high level of security. The tubes are composed of longitudinally welded beams to enable the installation of transverse beams, thus adding great strength to the structure.

The first rotor was positioned at the bow of the platform, and the position of the second rotor was obtained through the application of Newton's first law and an analysis of the trail produced by the first rotor.

OUTPUT OF THE WIND TURBINE

The power available to the rotor from the wind is calculated using Eq. (1), which expresses the power as a proportion of the swept area and the cube of the wind speed, v:

$$P_{wind} = \frac{1}{2} \cdot \rho \cdot A \cdot v^3 \quad (1)$$

Not all of the kinetic energy of the wind can be converted into rotational mechanical energy, as shown in Eq. (2). The final power is limited by several elements that represent different losses in the process of converting wind energy into electrical energy. The power coefficient C_p is called the efficiency of the turbine, and its value cannot exceed Betz's limit of 59.3% [15].

$$P_{mech} = C_p \cdot P_{wind} = C_p \cdot \frac{1}{2} \cdot \rho \cdot A \cdot v^3 \quad (2)$$

A typical efficiency C_p for a Savonius rotor is 20–24%, and depends on the specific configuration, for example the values of s/D and L/H (see Fig. 1), the number of blades, and the Reynolds number *Re*. In the current work, *Re* = 274,126 for a wind velocity v = 8 m/s.

C_p is not constant, but varies with the wind speed, the angular velocity of the turbine, the number of the rotor blades and the shape of the guide vane. These characteristics strongly affect the blockage that the wind turbine produces in the air flow.

Another way to specify the efficiency of a wind turbine is in terms of a tangential speed ratio (also known as tip speed ratio) or TSR, as shown in Eq. (3). This term replaces the number of revolutions per minute n for the turbine, and is used to compare the performance of wind machines. The TSR is a good metric for analysing the C_p behaviour of a given type of wind turbine.

$$\text{TRS} = \frac{r_{aero} \cdot \omega_{aero}}{v} \quad (3)$$

where r_{aero} is the radius of the wind turbine, ω_{aero} is its angular velocity, and v is the wind speed.

A numerical model (CFD) was created to determine the characteristics of dimensionless power C_p and compared with experimental data (EXP) [23], as shown in Figure 3, for different Reynolds numbers. The Reynolds number was defined based on varying inflow velocities (RUN 57 - 7 m/s, RUN 58 - 14 m/s. A comparison of the results showed no significant qualitative differences between CFD and EXP data. The numerical results were positively verified by experiment, and in this work, the same approach is applied at the model's preparation stage with guide vanes.

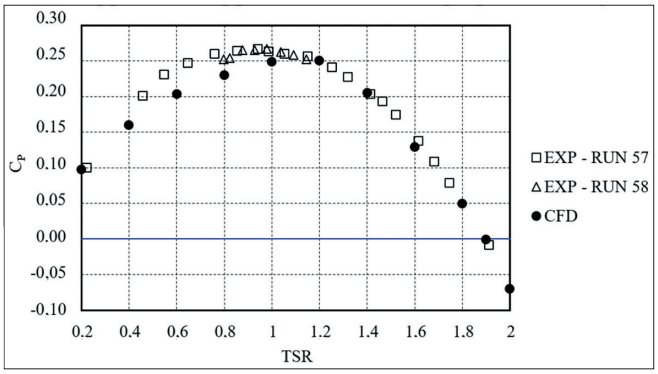

Fig. 3. CFD power curve and comparison with experimental results [23]

PLATFORM DESIGN

There was a gap in the deck of the real catamaran, as shown in Fig. 4(a). The pontoons and the main deck were fixed together, and the assembled result is presented in Fig. 4(b).

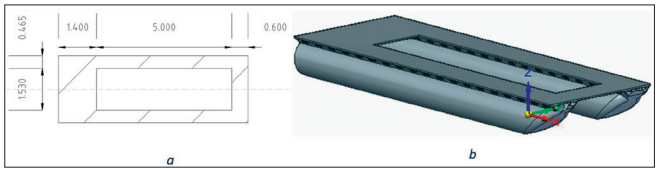

Fig. 4. (a) Deck with hole; (b) pontoons with the main deck (all dimensions in metres)

INITIAL ESTIMATION OF THE CENTRE OF GRAVITY

In the next step, the centre of gravity of the empty platform was estimated. In these calculations, we assumed that the platform was composed of a deck and two pontoons (cylinders).

The centre of gravity is defined as:

$$\vec{Z}_G = \frac{\Sigma W_k \cdot \vec{r}_k}{W_{platform}} \quad (4)$$

where W_k is the weight of each element making up the platform, $\vec{r}_k$ is a vector that describes the distance between the centre of gravity of each element and the established origin of the coordinate system, and $W_{platform}$ is the total weight of the platform (484 kg). The vectors $\vec{r}_k$ represent a centre of gravity for each individual element, as shown in Eq. (5).

$$\vec{Z}_G = \frac{W_{cone1} \cdot \vec{r}_{cone1} + W_{cone2} \cdot \vec{r}_{cone2} + W_{cyl1} \cdot \vec{r}_{cyl1} + W_{cyl2} \cdot \vec{r}_{cyl2} + W_{deck} \cdot \vec{r}_{deck}}{W_{platform}} \quad (5)$$

For simplicity, the deck made of crossed beams is assumed to be a homogeneous cuboid of dimensions (7 × 2.46 × 0.025) m^3 and weight 260.65 kg. We also assume that the cones of the pontoons are straight rather than inclined. The origin of the coordinate system is shown in Fig. 5, and coincides with the bottom of the pontoons. Finally, the centre of gravity of the empty platform is $\boldsymbol{Z_G} = (Z_{Gx}; Z_{Gy}; Z_{Gz}) = (0.52; 0.55; 0)$ m.

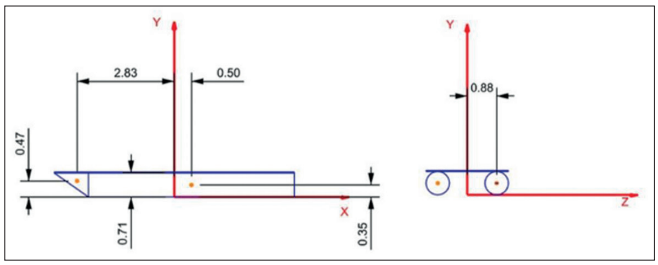

Fig. 5. Distances between components with the coordinate system in red (all dimensions in metres)

MOUNTING OF THE SAVONIUS ROTOR

When the main structure of the ship had been obtained, it was necessary to mount the Savonius rotor. The main idea for the installation of the rotor was to rotate its coordinate system

through 90°, to act as a horizontal turbine. The dimensions of this rotor are shown in Fig. 6, where T = 1 m, G = 0.1 m, L = 4.3 m, R = 0.5 m, and H = 1.25 m.

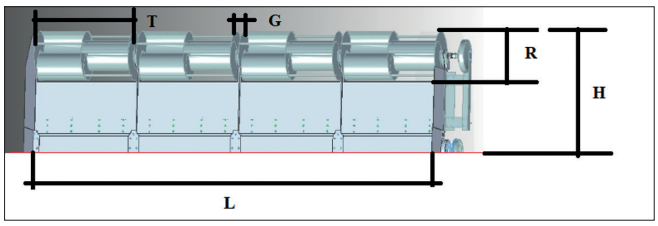

Fig. 6. Dimensions of the Savonius rotor

After cutting the initial rotor to obtain two smaller rotors, we needed to determine where they should be located along the platform. The first rotor was positioned at the fore of the platform. To determine the position of the second rotor, we monitored the trail from the first rotor using a simulation carried out in TASK. The parameters for the simulation of the first rotor were as follows: atmospheric pressure P_∞ = 101,325 Pa, TSR λ = 1, wind velocity U_{inf} = 8 m/s, rotor diameter R = 0.5 m, rotor's angular velocity ω = 32 1/s, time step 0.001091 s. The simulation results for the trail coming from the first rotor are shown in Fig. 7. The distance between the centre of the first rotor and the highest point of the trail is 1.2 m, and we need to add 0.25 m to this value to reach the centre of the second rotor, i.e. $D_{between\ centres}$ = 1.2 + 0.25 = 1.45 m. The total height of the second rotor is therefore:

$$H_{sec\ rotor}=D_{between\ centres}+H+R=1.45+1.25+0.25=2.70\ \text{m} \quad (6)$$

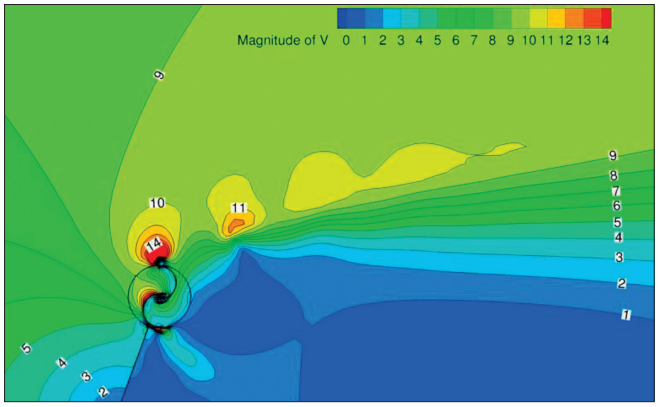

Fig. 7. Simulation results for the trail from the first rotor

FINAL ESTIMATION OF THE CENTRE OF GRAVITY, BUOYANCY AND METACENTRIC HEIGHT

The centre of ***gravity*** of the platform with rotors is defined as:

$$\vec{Z}_G = \frac{\Sigma W_k \cdot \vec{r}_k}{W_{total}} \quad \text{where} \quad \vec{r}_k = (r_x, r_y, r_z) \quad (7)$$

$$Z_G = \frac{W_{platform} \cdot Z_{Gplatform} + W_{total\,rotor1} \cdot Z_{Gtotal\,rotor1} + W_{total\,rotor1} \cdot Z_{Gtotal\,rotor1}}{W_{total}} \quad (8)$$

were $W_{total} = W_{platform} + W_{total\,rotor1} + W_{total\,rotor2}$

The weight of the rotors and their supports was estimated using the Autodesk Inventor programme as follows: Rotor 1 = 180 kg, Support 1 = 85 kg, Rotor 2 = 180 kg, Support 2 = 150 kg. These values give the weights of the two whole rotors with their supports as: $W_{total\,rotor1}$ = 265 kg, $W_{total\,rotor2}$ = 330 kg. Since the weight of the platform (two pontoons with deck) is 484 kg, we can establish the total weight as W_{total} = 1079 kg. For simplification, the centre of gravity of each rotor was treated as a cuboid. As follows from the first principle of Newton's dynamics, the whole platform is in equilibrium when the resultant moment of force is zero, giving values of x_1 = −3.06 m, x_2 = 2.45 m. The values of the vectors for both rotors are shown in Table 1.

Tab. 1. Component vectors for the rotors

$\vec{r}_{rotor1}$	x	–3.06	m
	y	1.31	m
	z	0	m
$\vec{r}_{rotor2}$	x	2.45	m
	y	2.08	m
	z	0	m

Finally, we obtain the centre of gravity of the whole platform, together with rotors as $\mathbf{Z_G} = (Z_{Gx}; Z_{Gy}; Z_{Gz})$ = (0.23; 1.2; 0) m. A 3D model of the platform with the rotors on board is shown in Fig. 8.

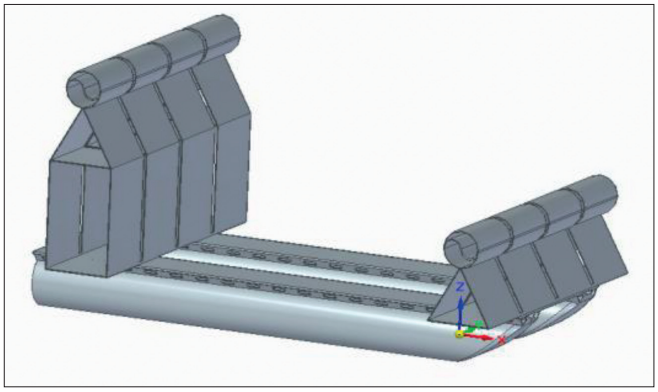

Fig. 8. Final 3D model

To calculate the centre of ***buoyancy***, we need to know the draught of the platform when the rotors are installed. A mathematical description of this issue can be found in [16]. In this case, we can apply Archimedes' principle, and to simplify the calculations, we consider the cones as an extension of the cylinders. For a floating platform, Archimedes' principle is formulated as:

$$m_b \cdot g = \rho_w \cdot g \cdot V_b \quad (9)$$

where m_b is the mass of fluid displaced, g is the gravitational constant, ρ_w is the density of the water in which the platform is immersed, and V_b is the displaced volume of the platform.

The ***draught*** of the platform, calculated using the equation for a circular segment [17], is equal to T = 0.2 m. Hence, when the platform is in water, the immersed part of each pontoon is smaller than its radius (0.35 m).

When the draught had been calculated, the centre of buoyancy was determined as follows:

$$\vec{Z}_B = \frac{\Sigma V_k \cdot \vec{r}_k}{V_{total}} \tag{10}$$

$$\vec{Z}_B = \frac{V_{pontoon1} \cdot \vec{r}_{pontoon1} + V_{pontoon2} \cdot \vec{r}_{pontoon2}}{V_{total}} \tag{11}$$

where V_k is the immersed volume, $\vec{r}_k$ is a vector representing the distance between the centre of gravity of the immersed volume and the established coordinate system, and V_{total} is the total immersed volume. The centre of buoyancy of the single immersed pontoon is given in Eq. (12):

$$\vec{r}_{pontoon1,\,2} = x \cdot \hat{x} + y \cdot \hat{y} + z \cdot \hat{z} \tag{12}$$

were $x = 0,\ y = \frac{4 \cdot T}{3 \cdot \pi} = 0.11\ m,\ z = 0.88\ m$ for Pontoon 1
and $x = 0,\ y = \frac{4 \cdot T}{3 \cdot \pi} = 0.11\ m,\ z = -0.88\ m$ for Pontoon 2

Eq. (13) gives the centre of buoyancy for the whole platform:

$$x = 0\ m,\ y = \frac{4 \cdot T}{3 \cdot \pi} = 0.11\ m,\ z = 0 \tag{13}$$

The ***transversal metacentric height*** is defined as shown in Eq. (14) [18]:

$$GM = Z_B + \mathrm{BM} - Z_G \tag{14}$$

Here, BM is the metacentric radius and is defined as $BM = \frac{I}{\nabla}$, where ∇ is the immersed volume of the two pontoons, and I is the moment of inertia, which is calculated in different ways depending on the coordinate system used. We select the x-axis to calculate the metacentric radius. From Steiner's theorem [19] and few calculations, we obtain values of ***BM* = 6.38 m** and ***GM* = 5.97 m**. The platform is stable when $GM > 1$. If the metacentre lies above the centre of gravity, a righting moment is produced, the equilibrium is stable and the metacentre height is regarded as positive. This condition is fulfilled for our platform, and it can therefore be considered as stable.

ANCHORING SYSTEM

The anchoring system is used to fix the platform to the bottom of the sea or lake. The wind and waves will exert a certain force on the 'living work' (non-immersed part) of the platform. In addition, the current exerts a force on the 'dead work' (immersed part) of the platform. The resulting force must be withstood by our anchoring system.

The goal of this part of the project is the selection of the anchor and mooring line. In our platform, four fixed bars are installed in the centre hole of the platform, and are joined at the centre point as shown in Fig. 9(a).

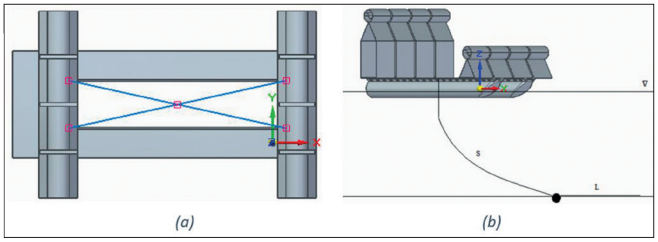

Fig. 9. Arrangement of the anchoring system

At the point at which the bars meet, we attach the first link of the anchor line. The anchor line extends to the bed over the depth of the lake as shown in Fig. 9(b). This system allows a swinging circle (Fig. 10) to be produced, in which the platform will be able to pivot around the anchor due to the effects of the wind or current. This arrangement allows the rotors to face the maximum wind direction, meaning that the output of these rotors will be the greatest and the turbine will be most efficient.

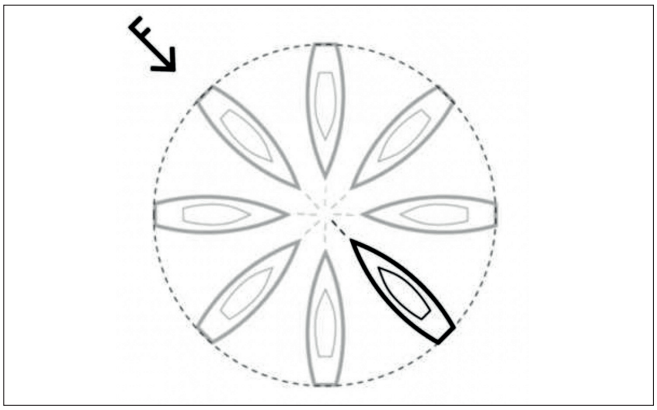

Fig. 10. Swinging movement of the platform

CALCULATION OF THE ANCHORING SYSTEM

The anchor is essential equipment in order to restrain the device. The choice of anchor weight is mainly based on the length of the platform. A correct selection of the weight will prevent the chain from breaking due to the force that it has to withstand caused by pulling of the platform. To carry out our calculations, we use a document called *Part III: Hull Equipment* from the PRS classification society and draw on the study in [20]. The weight of the anchor is calculated with the following formula:

$$W_a = k \cdot B \cdot T(kg) \tag{15}$$

where B is the maximum beam on board (in metres), T is the draught, and $k = c \cdot \sqrt{\frac{L}{8 \cdot B}}$ for a pushed barge, where c is the empirical coefficient adopted in accordance with [21]. L is the maximum length on board. The value used for our platform are shown in Table 2.

Tab. 2. Values used for the anchor weights

L*	7.4	m
B**	4.3	m
T	0.2	m
c	45	–
k	20.9	–

* The length is the maximum length including the auxiliary systems of the ship.
**The beam is the maximum width of the rotor.

The weight of the anchor, according to the formula (15) is around 31 kg, but in this case it is assumed to be $W_a = 100$ kg. This assumption is made because when adding a weight greater than the calculated one, we must be sure that the fixed anchor has

a greater gripping power on the seabed and thus the platform does not move under any conditions once the anchor is working, and the chances of grabbing will be at a minimum. To check whether the estimated anchor weight is sufficiently large, we must calculate the weight using Eq. (15). This formula gives W_a = 18 kg, which is much smaller than the assumed anchor weight.

The ***chain breaking*** load is defined as:

$$R = 0.35 \cdot W_a \tag{16}$$

and is equal to R = 35 kg. The second element of the anchoring system is the ***length of the chain***, which is calculated as:

$$L_C = K \cdot \sqrt{H} \tag{17}$$

where H = 5 m is the average water depth, and K is the coefficient, which depends on the type of steel used to manufacture the chain. For high-strength steel (forged steel), its value is K = 86.2, giving a chain length of L_C = 87 m.

One of the most important characteristics of an anchor is its ability to strongly attach to different types of bottom surfaces, i.e., its ability to hold up under loads (holding force) and its durability. The ***total anchor holding force*** is defined as:

$$L_{AHF} = F_a + F_C \tag{18}$$

where $F_a = W_a \cdot \lambda_a$ = 0.34 t is the holding power of the anchor, and λ_a = 8 (taken from [20]) is the only anchor keeping force in sea bottom soil. F_C is the chain holding force (in tons).

Before calculating the holding force, a chain was selected from the catalogue in [22]. The selected chain had the characteristics shown in Fig. 11.

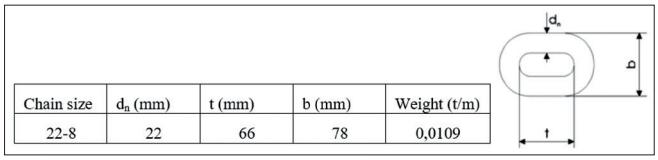

Chain size	d_n (mm)	t (mm)	b (mm)	Weight (t/m)
22-8	22	66	78	0,0109

Fig. 11. Characteristics of the selected sling chain, which is in strength class "8" according to EN 818-2 [22]

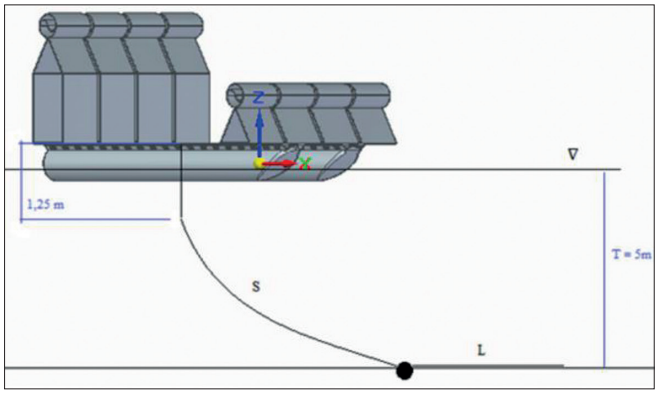

Fig. 12. Arrangement of the anchoring system

The chain holding force is given in Eq. (19), and the arrangement of the anchor is shown in Fig. 12.

$$F_C = W_S \cdot \lambda_S + W_L \cdot \lambda_L \tag{19}$$

where $W_S = L_S \cdot 0.0109$ is the suspended chain weight (t), L_S is the suspended chain length (where we assume that 7 m of the chain are suspended in water), and λ_S is the suspended chain coefficient.

$W_L = L_L \cdot 0.0109$ is the weight of the chain lying on the bottom (t), where $L_L = L_C - L_S$ = 80 m is the length of the lying chain. λ_L is the lying chain coefficient. The values of the coefficients and chain weights are shown in Table 3.

Tab. 3. Data used to calculate the chain holding force

λ_a	0.87	–
W_S	0.076	t
λ_L	1	–
W_L	0.872	t

Finally, we obtain the chain holding force as F_C = 0.94 t.

The total anchor holding force is F_{AHF} = 1.28 t. This force must be greater than the environmental force. To check that the proposed mooring system is valid, the environmental forces must be calculated. In units of t, we can calculate the environmental force by dividing Eq. (1) by a maximum velocity of 60 m/s, which gives F_{env} = 1.21 t. This means that $F_{AHF} > F_{env}$, and hence the environmental force is smaller than the total anchor holding power.

CONCLUSION

The wind turbine used in this project was a Savonius rotor, and the characteristic force and power available from the wind were analysed. We considered wind speeds ranging from zero to those that can be found under the action of a hurricane.

A typical large Savonius rotor was replaced by an innovative wind turbine with a thrust plate and a small rotor at the tip of this plate. The overall system of thrust plate and rotor was implemented as a horizontal-axis wind turbine, and delivered as much energy as a large Savonius rotor. This new design is less demanding in terms of manufacturing and costs. The possibility of directing the rotors against the wind was achieved by using a floating solution, consisting of a catamaran composed of 7 m length pontoons.

To ensure that the rotor gave the maximum possible performance, two Savonius wind turbines were installed on board. We assumed that the first rotor was located at the bow of the platform, and the position of the second rotor is obtained through the application of Newton's first law and an analysis of the trail produced by the first rotor.

The centre of gravity, the centre of buoyant force and the metacentric height were calculated, and it was confirmed that the whole system was stable.

Finally, an anchoring system was selected for the innovative floating wind turbine. In this design, the floating platform is anchored to the lake bottom, allowing for 360° rotation. The

proposed system will therefore position itself against the wind current, meaning that the rotors are in the most efficient position to capture wind. The selected mooring system is designed for the maximum speed of 60 m/s.

REFERENCES

1. Dymarski P. Design of jack-up platform for 6 MW wind turbine: Parametric analysis based dimensioning of platform legs. Polish Maritime Research 26:183-197, 2019. DOI: 10.2478/pomr-2019-00382.

2. Żywicki J, Dymarski P, Ciba E, Dymarski C. Design of structure of tension leg platform for 6 MW offshore wind turbine based on FEM analysis. Polish Maritime Research 24(s1):230-241, 2017. DOI: 10.1515/pomr-2017-00433.

3. Dymarski P, Dymarski C, Ciba E. Stability analysis of the floating offshore wind turbine support structure of cell spar type during its installation. Polish Maritime Research 26, 4(104):109-116, 2019. DOI: 10.2478/pomr-2019-0072.

4. Ciba E, Dymarski P, Grygorowicz M. Analysis of the hydrodynamic properties of the 3-column spar platform for offshore wind turbines. Polish Maritime Research 29:35-42, 2022. DOI: 10.2478/pomr-2022-0015.

5. Santhakumar S, Palanivel I, Venkatasubramanian K. A study on the rotational behaviour of a Savonius wind turbine in low rise highways during different monsoons. Energy for Sustainable Development 40:1-10, 2017.

6. Jia R, Xia H, Zhang S, Su W, Xu S. Optimal design of Savonius wind turbine blade based on support vector regression surrogate model and modified flower pollination algorithm. Energy Conversion and Management 270(5):116247, 2022, DOI: 10.1016/j.enconman.2022.116247.

7. Naik S K, Sachar S, Ianakiev A. Performance analysis of low Reynolds number vertical axis wind turbines using low-fidelity and mid-fidelity methods and wind conditions in the city of Nottingham. Energy. 279:127904, 2023, DOI: 10.1016/j.energy.2023.127904127904.

8. Al-Bahadly I. Building a wind turbine for rural home. Energy for Sustainable Development 13(3):159-165, 2009.

9. Akwa J V, Alves da Silva Jr. G, Prisco Petry A. Discussion on the verification of the overlap ratio influence on performance coefficients of a Savonius wind rotor using computational fluid dynamics. Renewable Energy 38(1):141-149, 2012. DOI: 10.1016/j.renene.2011.07.013.

10. Sukanta R, Antoine Ducoin D. Unsteady analysis on the instantaneous forces and moment arms acting on a novel Savonius-style wind turbine. Energy Conversion and Management 121:281-296, 2016. DOI: /10.1016/j.enconman.2016.05.044.

11. Doerffer K, Telega J, Doerffer P, Hercel P, Tomporowski A. Dependence of power characteristics on Savonius rotor segmentation. Energies 14:2912, 2021. DOI: 10.3390/en14102912.

12. Sachar S, Doerffer P, Flaszynski P, Kotus J, Doerffer K, Grzelak J. Correlation between the generated noise and effectiveness for a vertical axis Savonius type rotor. In AIAA SCITECH 2023 Forum, p. 0611, 2023. DOI: 10.2514/6.2023-0611.

13. Doerffer P, Doerffer K, Ochrymiuk T, Telega J. Variable size twin-rotor wind turbine. Energies 12:2543, 2019. DOI:10.3390/en12132543.

14. A traditional Savonius rotor. Retrieved from https://www.researchgate.net/figure/A-traditional-Savonius-rotor-46_fig8_322845539.

15. Betz A. Introduction to the theory of flow machines. (D. G. Randall, Trans.). Pergamon Press; 1966.

16. Journee J M M, Massie W W. Offshore hydromechanics. Delft University of Technology; 2001.

17. Beyer W H (Ed.). CRC standard mathematical tables, 28th ed. CRC Press; 1987.

18. Comstock J. Principles of naval architecture. Society of Naval Architects and Marine Engineers; 1967.

19. Haas A E. Introduction to theoretical physics. Van Nostrand; 1928.

20. Jurdziński M. Planowanie Kotwiczenia Dużych Statków Na Głębokich Kotwicowiskach. Zeszyty Naukowe Akademii Morskiej w Gdyni, nr 92, 2015. [Anchor Planning for Large Vessels in Deep Anchorages - Scientific Notebooks]

21. Rules for the classification and construction of sea-going ships, Part III: Hull equipment. PRS; 2023.

22. KIM Liny i Zawiesia. Retrieved from https://linystalowe.pl/oferta/łańcuchy/. [Ropes and slings]

23. Sheldahl, R.E., Feltz, L.V., Blackwell, B.F., 1978. Wind tunnel performance data for two- and three-bucket Savonius rotors. J. Energy 2:160-164. ttps://doi.org/10.2514/3.47966.